JCI The Journal of Clinical Investigation

Nkx3.1 and Myc crossregulate shared target genes in mouse and human prostate tumorigenesis

Philip D. Anderson, … , Isam-Eldin Eltoum, Sarki A. Abdulkadir

J Clin Invest. 2012;122(5):1907-1919. https://doi.org/10.1172/JCI58540.

Research Article **Oncology**

Cooperativity between oncogenic mutations is recognized as a fundamental feature of malignant transformation, and it may be mediated by synergistic regulation of the expression of pro- and antitumorigenic target genes. However, the mechanisms by which oncogenes and tumor suppressors coregulate downstream targets and pathways remain largely unknown. Here, we used ChIP coupled to massively parallel sequencing (ChIP-seq) and gene expression profiling in mouse prostates to identify direct targets of the tumor suppressor Nkx3.1. Further analysis indicated that a substantial fraction of Nkx3.1 target genes are also direct targets of the oncoprotein Myc. We also showed that Nkx3.1 and Myc bound to and crossregulated shared target genes in mouse and human prostate epithelial cells and that Nkx3.1 could oppose the transcriptional activity of Myc. Furthermore, loss of Nkx3.1 cooperated with concurrent overexpression of Myc to promote prostate cancer in transgenic mice. In human prostate cancer patients, dysregulation of shared NKX3.1/MYC target genes was associated with disease relapse. Our results indicate that NKX3.1 and MYC coregulate prostate tumorigenesis by converging on, and crossregulating, a common set of target genes. We propose that coregulation of target gene expression by oncogenic/tumor suppressor transcription factors may represent a general mechanism underlying the cooperativity of oncogenic mutations during tumorigenesis.

Nkx3.1 and Myc crossregulate shared target genes in mouse and human prostate tumorigenesis

Philip D. Anderson,[1] Sydika A. McKissic,[1] Monica Logan,[2] Meejeon Roh,[1] Omar E. Franco,[3] Jie Wang,[1] Irina Doubinskaia,[1] Riet van der Meer,[1] Simon W. Hayward,[3,4] Christine M. Eischen,[1,4] Isam-Eldin Eltoum,[5] and Sarki A. Abdulkadir[1,4]

[1]Department of Pathology, Microbiology and Immunology, Vanderbilt University Medical Center, Nashville, Tennessee, USA. [2]Department of Biochemistry and Cancer Biology, Meharry Medical College, Nashville, Tennessee, USA. [3]Department of Urology and [4]Department of Cancer Biology, Vanderbilt University Medical Center, Nashville, Tennessee, USA. [5]Department of Pathology, University of Alabama at Birmingham, Birmingham, Alabama, USA.

Cooperativity between oncogenic mutations is recognized as a fundamental feature of malignant transformation, and it may be mediated by synergistic regulation of the expression of pro- and antitumorigenic target genes. However, the mechanisms by which oncogenes and tumor suppressors coregulate downstream targets and pathways remain largely unknown. Here, we used ChIP coupled to massively parallel sequencing (ChIP-seq) and gene expression profiling in mouse prostates to identify direct targets of the tumor suppressor Nkx3.1. Further analysis indicated that a substantial fraction of Nkx3.1 target genes are also direct targets of the oncoprotein Myc. We also showed that Nkx3.1 and Myc bound to and crossregulated shared target genes in mouse and human prostate epithelial cells and that Nkx3.1 could oppose the transcriptional activity of Myc. Furthermore, loss of Nkx3.1 cooperated with concurrent overexpression of Myc to promote prostate cancer in transgenic mice. In human prostate cancer patients, dysregulation of shared NKX3.1/MYC target genes was associated with disease relapse. Our results indicate that NKX3.1 and MYC coregulate prostate tumorigenesis by converging on, and crossregulating, a common set of target genes. We propose that coregulation of target gene expression by oncogenic/tumor suppressor transcription factors may represent a general mechanism underlying the cooperativity of oncogenic mutations during tumorigenesis.

Introduction

Classic studies showed that malignant transformation is crucially dependent on cooperative interactions between distinct oncogenic mutations (1, 2). In a model of Ras/p53-mediated transformation, cooperativity between oncogenic mutations was shown to be mediated by the synergistic coregulation of a class of targets called cooperation response genes, which are important for tumorigenicity (3). Presently, it is unknown whether coregulation of multiple cancer-related target genes by cooperating oncogenic mutations is a generalized process in carcinogenesis (4). Furthermore, the potential mechanism or mechanisms by which alterations in specific oncogenes/tumor suppressor genes (TSGs) may lead to a cooperative response in target gene expression are not clear. In principle, for oncogenes/TSGs that encode transcription factors, direct coregulation of target gene expression might provide a mechanistic explanation for cooperativity. Here, we present our analysis of genome-wide binding sites for the prostate tumor suppressor and transcriptional regulator Nkx3.1, which led us to discover an interaction between Nkx3.1 and the oncoprotein Myc. We show that Nkx3.1 and Myc directly regulate a set of shared target genes and cooperate in prostate tumorigenesis.

Nkx3.1 is a homeodomain-containing transcription factor with roles in prostate development and cancer (5). Recent studies indicate that Nkx3.1 marks a population of castration-resistant luminal stem cells and is required for stem cell self renewal (6). Nkx3.1 protein is commonly attenuated in mouse and human prostate tumors (7, 8), and a germ line sequence variant that impairs NKX3.1 DNA binding has been associated with hereditary prostate cancer (9). More recently, Genome-Wide Association Studies (GWAS) identified a functional variant in *NKX3.1* associated with reduced gene expression as a risk factor for sporadic prostate cancer (10–12). Deletion of one or both alleles of *Nkx3.1* in mice leads to epithelial hyperplasia, dysplasia, and low-grade prostatic intraepithelial neoplasia (LGPIN) (13, 14). Introduction of additional mutations, such as deletion of a single allele of the *Pten* TSG, promotes the progression of the premalignant lesions in *Nkx3.1*$^{-/-}$ and *Nkx3.1*$^{+/-}$ mice to invasive carcinoma with metastasis (15, 16). Conversely, in a conditional *Pten*-deletion model of prostate cancer, Nkx3.1 expression was uniformly lost, and reconstituting Nkx3.1 expression by lentiviral-mediated gene transfer into *Pten*-deficient cells potently suppressed tumorigenicity (17, 18). Thus, a wealth of evidence suggests that reductions in the amount of Nkx3.1 protein may be permissive for prostate cell transformation.

Despite the critical role played by Nkx3.1 in prostate development and cancer, we know very little about the sites bound by this transcription factor in vivo or the genes and pathways it regulates. To obtain a comprehensive view of the genes and pathways regulated by Nkx3.1 in the prostate, we employed ChIP coupled with massively parallel sequencing (ChIP-seq) to identify Nkx3.1-binding sites across the genome (the Nkx3.1 "cistrome"). We integrated the ChIP-seq data with gene expression profiling to identify "direct" Nkx3.1 target genes that are both bound and regulated

Authorship note: Philip D. Anderson and Sydika A. McKissic contributed equally to this work.

Conflict of interest: The authors have declared that no conflict of interest exists.

Citation for this article: *J Clin Invest.* 2012;122(5):1907–1919. doi:10.1172/JCI58540.

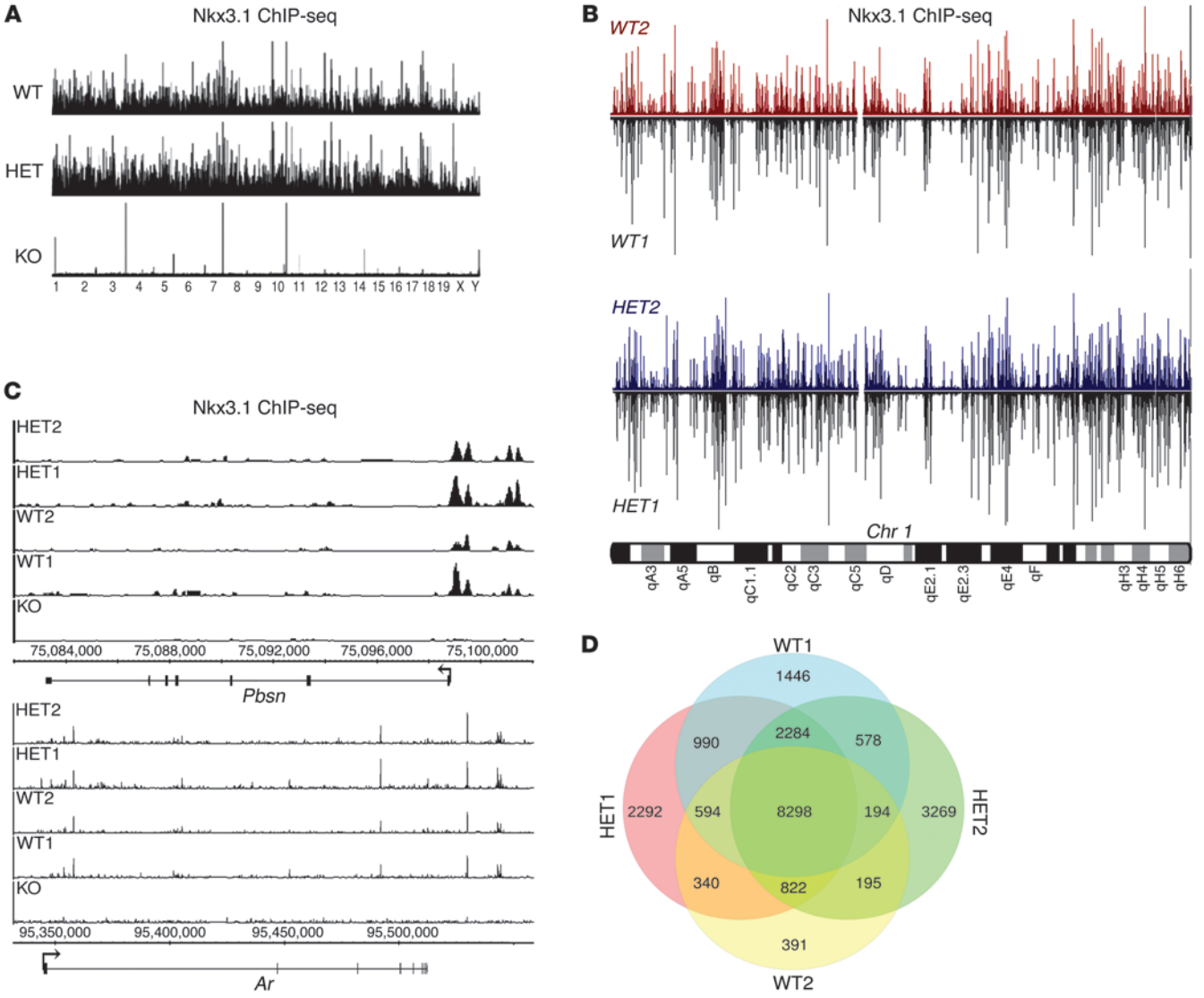

Figure 1

Analysis of genome-wide Nkx3.1-binding sites in the mouse prostate. (**A**) Visualization of Nkx3.1-binding sites across all mouse chromosomes in *Nkx3.1*$^{+/+}$ (WT), *Nkx3.1*$^{+/-}$ (HET), and *Nkx3.1*$^{-/-}$ (KO) mouse prostates. Not to scale. (**B**) High reproducibility in Nkx3.1-binding sites among biological replicates and genotypes. Chromosome 1 is shown as an example. (**C**) Integrated Genome Browser (IGB) shots showing Nkx3.1-binding sites near the *Pbsn* and *Ar* genes. (**D**) Euler diagram showing overlap of Nkx3.1-binding sites in WT and HET mouse prostates. See also Supplemental Figure 1 and Supplemental Table 1.

by Nkx3.1. We further used network analysis to identify potential connections between Nkx3.1 and other transcription factors in target gene regulation. Notably, a link to the protooncogene Myc was identified, suggesting functional interactions between Nkx3.1 and Myc. We used in vitro and in vivo studies to validate this interaction, showing coregulation of target gene expression and prostate tumorigenicity by Myc and Nkx3.1.

Results

The Nkx3.1 cistrome in mouse prostate. To define the Nkx3.1 cistrome, we performed ChIP-seq in adult mouse prostate. In the mouse prostate, Nkx3.1 expression is largely restricted to the luminal epithelial cell compartment (14, 15). Thus, interpretation of any signals obtained from Nkx3.1 ChIP-seq analysis of whole prostate tissue is not complicated by potential cell type–specific differences in Nkx3.1-binding patterns. We performed ChIP-seq in 2 *Nkx3.1*$^{+/+}$ (WT), 2 *Nkx3.1*$^{+/-}$ (heterozygote [HET]), and, as a biological negative control, 1 *Nkx3.1*$^{-/-}$ (KO) mouse prostates (14). We then used the MACS algorithm (19) to call peaks, which correspond to Nkx3.1-binding sites. Between 13.6 and 15.1 million sequence tags were uniquely mapped to the genome per sample (Supplemental Table 1; supplemental material available online with this article; doi:10.1172/JCI58540DS1).Inclusion of the KO sample as a control showed excellent specificity of the α-Nkx3.1 antibody used in this assay (Figure 1, A and C). The locations and amplitudes of peaks were strikingly similar between genotypes (WT vs. HET) and biological replicates. Similarity was also seen genome wide (Figure 1A) at the chromosomal level (Figure 1B) and at the level of

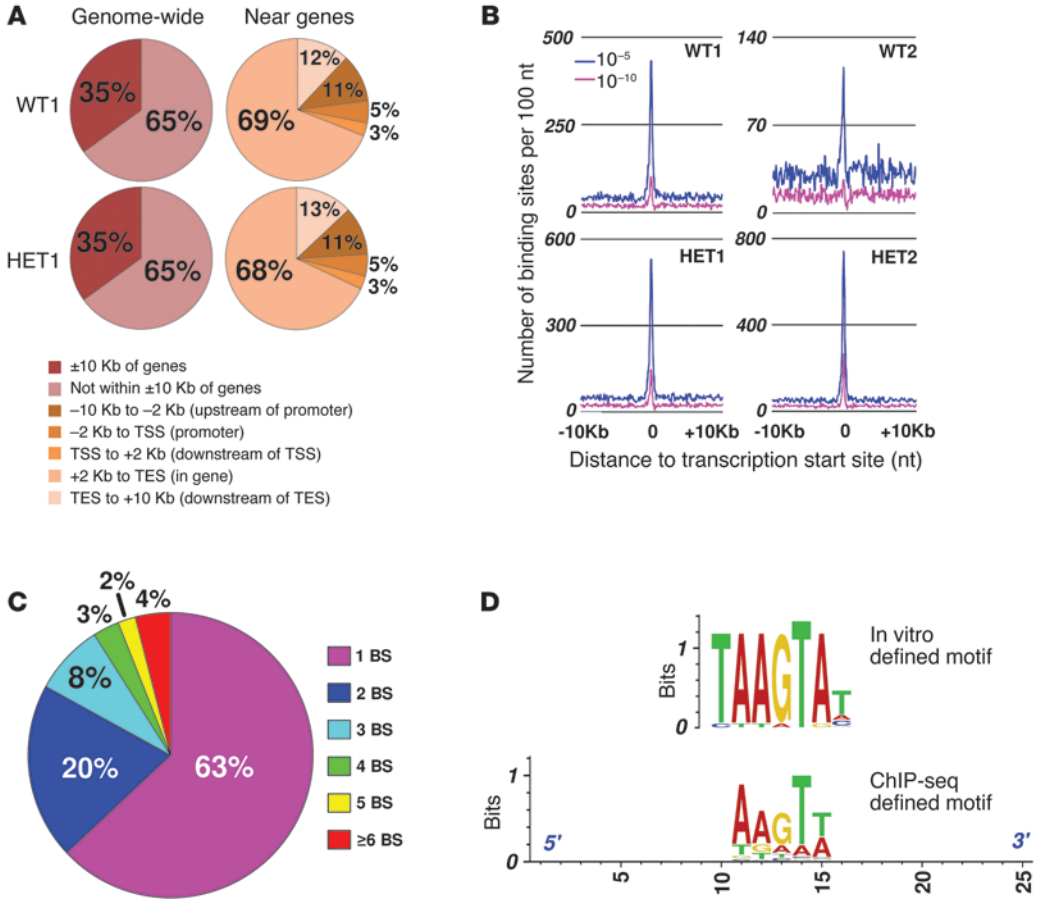

Figure 2

Analysis of the Nkx3.1 cistrome. (**A**) Spatial distribution of Nkx3.1 binding sites genome wide (red) or near genes as shown in the RefSeqGene database (http://www.ncbi.nlm.nih.gov/refseq/rsg/) (orange). The results from 1 WT prostate and 1 HET prostate are shown. (**B**) Enrichment of Nkx3.1-binding sites approximately 150 nt upstream of the TSS for all Nkx3.1-positive samples. Shown are results for MACS peak calling algorithm with the *P* value set at the default 10^{-5} and at 10^{-10}. (**C**) The number of times Nkx3.1 binds target genes is indicated. bs, binding site. (**D**) Top panel: in vitro defined Nkx3.1 motif (29). Bottom panel: consensus motif for Nkx3.1, as determined by querying the 1,000 most enriched ChIP-seq loci with MEME (v. 4.6.0). See also Supplemental Tables 2 and 3.

individual gene loci, such as the known Nkx3.1 target genes *Pbsn*, which encodes Probasin, and *Ar*, which encodes androgen receptor (Figure 1C and refs. 18, 20). These results demonstrate a high degree of reproducibility for the assay.

Nkx3.1-binding sites were generally evenly distributed across all chromosomes, with the lowest concentration of binding sites on the Y chromosome, even when the lower number of genes present on the Y chromosome was taken into account (Supplemental Figure 1A). Analysis of all bound genomic loci indicated that 8,298 (34.6%) were bound in all 4 Nkx3.1-expressing samples (Figure 1D and Supplemental Table 2). Overall, the HET samples had more binding sites than WT samples, which was contrary to our expectations, considering that reduction in *Nkx3.1* dosage is highly correlated with prostate tumorigenesis (5, 14, 21, 22). Since ChIP-seq yields a snapshot of cross-linked proteins bound to DNA, it may not be suitable for detecting dosage effects. The majority (65%) of Nkx3.1-bound intervals mapped within 10 kb of genes (Figure 2A and Supplemental Table 2), which was consistent with reports showing that other transcription factors prefer to bind in the vicinity of genes (23). The percentage of peaks mapping within 10 kb of genes was remarkably consistent across all 4 *Nkx3.1*-positive samples, ranging from 63% (WT2) to 66% (HET2) (Figure 2A and Supplemental Table 2). Promoter regions (–10 kb to +2 kb) contained 19% of all intervals that mapped within 10 kb of annotated genes. In contrast, 68% of intervals mapped between +2 kb and the transcription end site (TES) (Figure 2A and Supplemental Table 2). These data show a strong preference for Nkx3.1 binding in introns. We discovered a striking enrichment for Nkx3.1-binding sites approximately –150 nt upstream of the transcription start site (TSS) (Figure 2B). This enrichment was conserved across all 4 *Nkx3.1*-positive samples and was apparent even at a higher significance threshold ($P < 10^{-10}$) for peak calling.

Most Nkx3.1 target genes (63%) were bound once, while 20% were bound twice, 8% were bound 3 times, and 9% were bound 4 or more times (Figure 2C). We next examined for enrichment of known transcription factor DNA-binding motifs in the Nkx3.1-bound DNA fragments using Genomatix software (24). We found significant enrichment of several elements, including the NKX homeodomain consensus, which was present in 86% of sequences examined (Supplemental Table 3). Interestingly, the most enriched

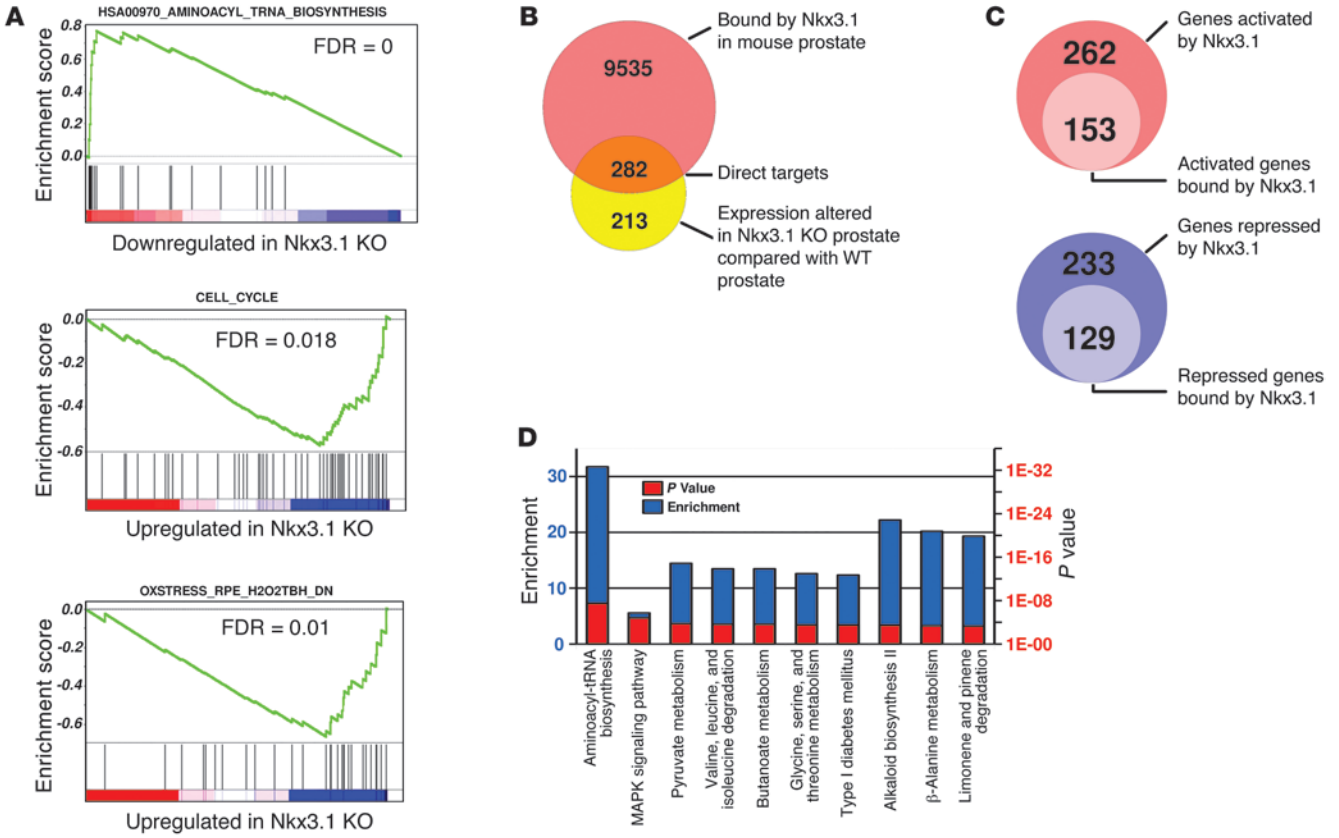

Figure 3

Identification of direct Nkx3.1 target genes. (**A**) GSEA analysis of genes whose expression is dysregulated in *Nkx3.1*$^{-/-}$ mice identifies significant downregulation of genes involved in aminoacyl tRNA synthesis and enrichment of genes involved in the cell cycle and oxidative stress in the KO mouse prostate. (**B**) Integration of Nkx3.1 ChIP-seq data with microarray analysis of *Nkx3.1*$^{-/-}$ mice identifies 282 direct Nkx3.1 target genes. (**C**) Venn diagrams showing the fraction of genes activated or repressed by Nkx3.1 that are also bound by Nkx3.1 by ChIP-seq, i.e., direct activated genes and direct repressed genes. (**D**) GO analysis of direct Nkx3.1 target genes by WebGestalt. See also Supplemental Figure 2 and Supplemental Table 4.

motif, occurring in 94% of the sequences, was the Forkhead consensus motif. Other enriched motifs included the GATA, Octamer, and TATA–binding factor motifs (Supplemental Table 3). Notably, several of these motifs were reported to be enriched in AR-bound fragments (25–28), although the androgen response element (ARE) was not among the top motifs identified by our analysis (Supplemental Table 3). A putative NKX3.1 DNA-binding motif has been previously defined in vitro using a selection and amplification binding (SAAB) assay (29). Identification of thousands of Nkx3.1-binding sites in our ChIP-seq analysis enabled us to refine the in vivo consensus Nkx3.1 motif. We queried MEME (30) with the 1,000 most enriched regions corresponding to the 1,000 most statistically significant binding sites identified by our ChIP-seq. The motif we discovered, AAGTW (Figure 2D), was similar but not identical to the NKX3.1-binding motif described in vitro, TAAGTA (29). The AAGTW motif was present in approximately 86% of all intervals (Supplemental Figure 1E).

Identification of direct Nkx3.1 target genes. We next sought to determine "direct" target genes that are both bound and regulated by Nkx3.1. We and others have previously used gene expression profiling to identify genes whose expressions are altered in the prostates of *Nkx3.1*-deficient mice (31, 32). To obtain further insight into gene expression changes in *Nkx3.1* KO versus WT prostates, we used Gene Set Enrichment Analysis (GSEA) (33) to reanalyze our microarray data (31). As shown in Figure 3A, we found dramatic changes in gene sets involved in aminoacyl tRNA synthesis, oxidative stress, and notably, cell cycle regulation (34, 35) in the KO prostates. These results reveal a regulatory role for Nkx3.1 in these processes. Next, we integrated our ChIP-seq data with the microarray data (31). We compared the 9,817 genes bound by Nkx3.1 in the ChIP-seq to the 495 genes changed in the microarray and identified 282 genes present in both lists. These "direct" Nkx3.1 target genes were both bound and regulated by Nkx3.1 (Figure 3B). Based on their expression patterns (i.e., upregulated or downregulated in KO), 153 of these genes were inferred to be activated and 129 to be repressed by Nkx3.1 (Figure 3C). Activated Nkx3.1 direct target genes included *Tmprss2*, *Prdx6*, *Gpx2*, and several *aminoacyl tRNA synthetase* genes (Supplemental Table 4). Repressed direct targets included *Angpt2*, *Hk2*, *Qsox1*, and *Nucb2* (Supplemental Table 4). Further analysis indicated that activation or repression by Nkx3.1 does not appear to be related to binding site location within the target genes (Supplemental Figure 2, A and B) or the number of bound sites per gene (P.D. Anderson and S.A. Abdulkadir, unpublished observations).

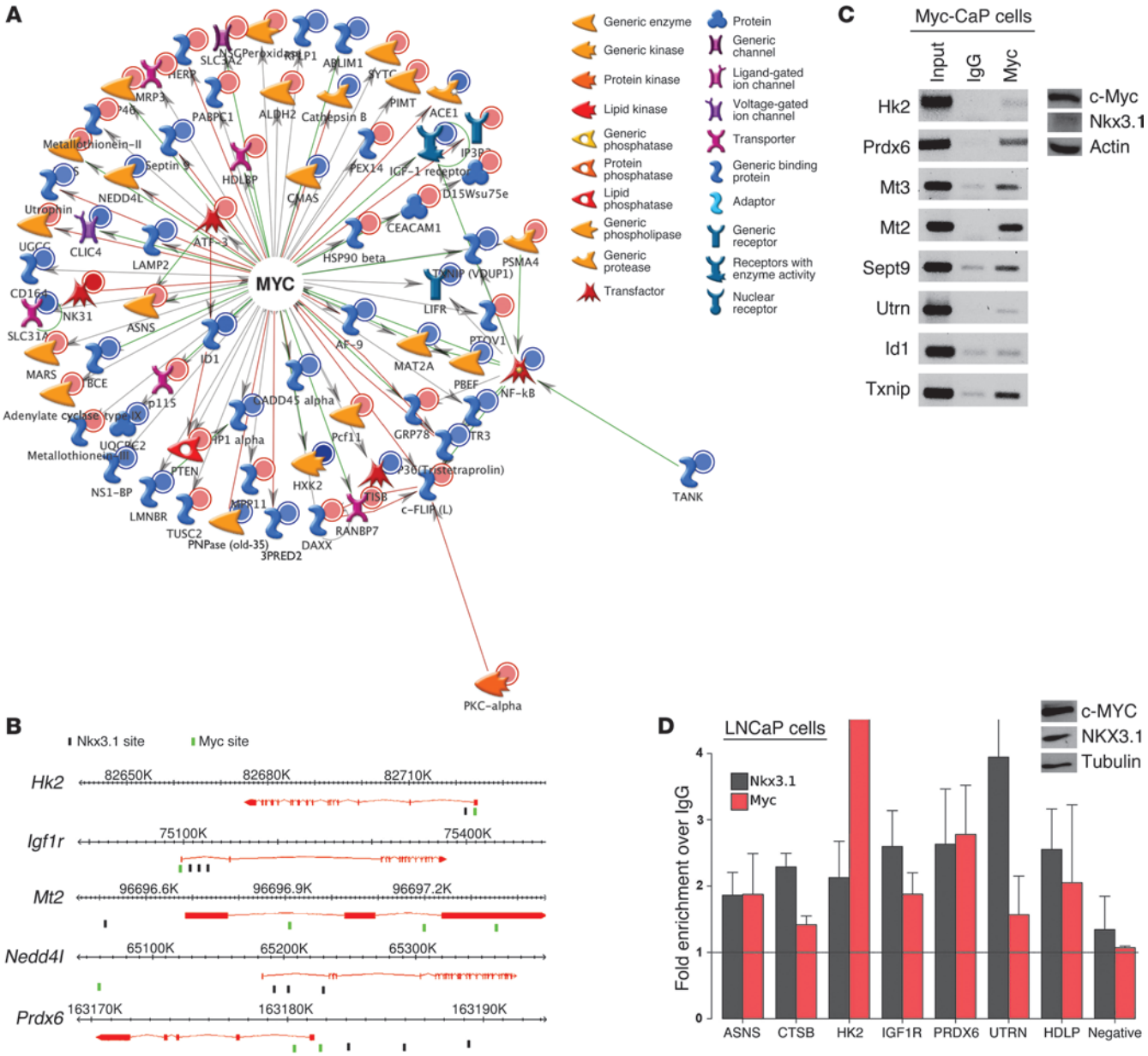

Figure 4

Identification of a subset of direct Nkx3.1 target genes coregulated by Myc. (**A**) Network analysis using GeneGO MetaCore software identifies a subset of direct Nkx3.1 target genes that are known to be bound by Myc ($P = 3.94 \times 10^{-169}$). Genes upregulated in the *Nkx3.1* KO prostates are shown as blue circles, while those downregulated are indicated as red circles in the diagram. (**B**) Relative locations of actual Nkx3.1- and Myc-binding sites in selected Nkx3.1/Myc coregulated genes identified from genome-wide binding studies. (**C**) ChIP-PCR validation of Myc binding to selected shared Nkx3.1/Myc target genes in Myc-CaP mouse prostate adenocarcinoma cell line (top). These cells express Myc but not Nkx3.1, as shown in the inset Western blot. Results are representative of at least 2 independent experiments. (**D**) ChIP-qPCR validation of MYC and NKX3.1 binding to selected shared NKX3.1/MYC target genes in LNCaP human prostate adenocarcinoma cell line. These cells express both MYC and NKX3.1, as shown in the inset Western blot. Results are presented as mean ± SD from at least 2 independent experiments. See also Supplemental Tables 5 and 6.

We used WebGestalt (36) to test for enrichment of gene ontology (GO) terms among the direct target genes (Figure 3D). Interestingly, genes labeled as components of the aminoacyl-tRNA synthesis pathway were the most enriched category of GO terms ($P < 3.0 \times 10^{-8}$, hypergeometric test), which corroborates the GSEA results predicting an important role for Nkx3.1 in the regulation of protein biosynthesis. Genes in the MAPK signaling pathway were also highly enriched in both the direct targets (Figure 3D) and the ChIP-seq targets overall (Supplemental Figure 1C), suggesting that dysregulation of MAPK pathway members may contribute to the prostate phenotype of *Nkx3.1*-deficient mice.

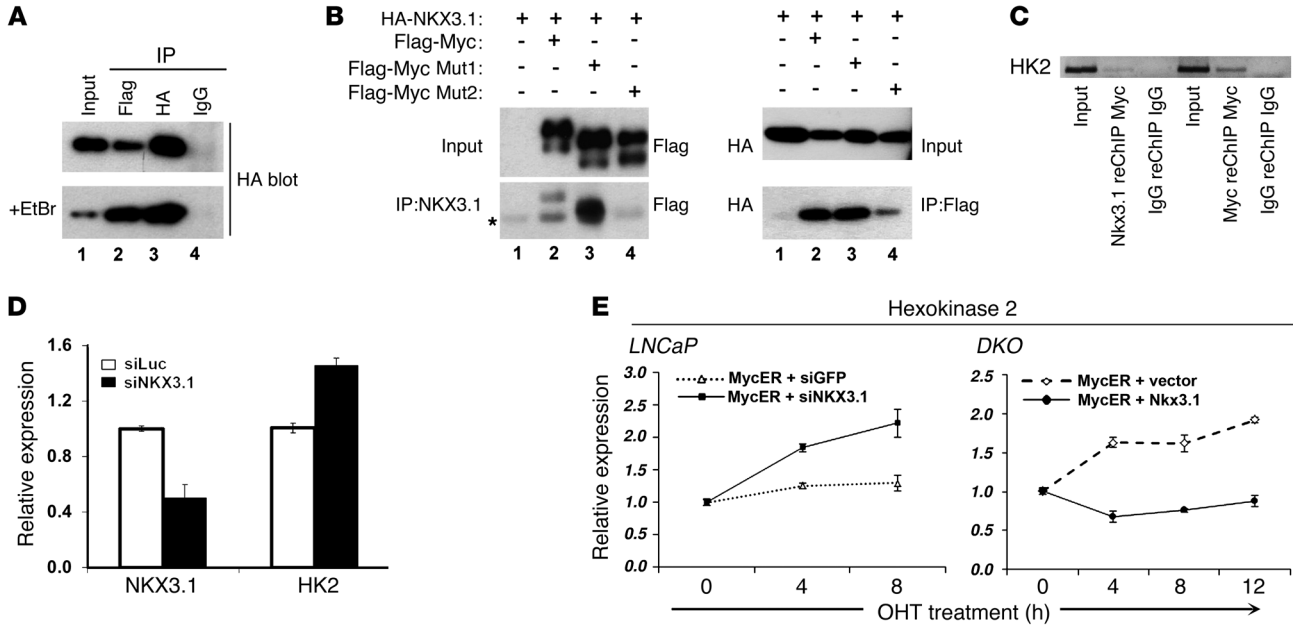

Figure 5

NKX3.1 and Myc interact and coregulate expression of shared target gene *HK2*. (**A**) Myc and NKX3.1 coimmunoprecipitation. Cell lysates from 293T cells expressing HA-NKX3.1 and Flag-Myc were immunoprecipitated with the indicated antibodies and immunoblotted for HA. To deplete DNA, ethidium bromide (EtBr) was added to lysates for 30 minutes prior to immunoprecipitation and during washes. (**B**) Coimmunoprecipitation of HA-NKX3.1 and Flag-Myc WT (lane 2), Flag-Myc mutant 1 lacking Myc–box 1 (lane 3), or Flag-Myc mutant 2 lacking Myc–box 2 (lane 4) in 293 cells. Asterisk indicates a nonspecific band. (**C**) ChIP–re-ChIP assay. LNCaP cells were subjected to ChIP by NKX3.1 antibody followed by ChIP with Myc antibody or the reverse and binding interrogated at the HK2 promoter E box. (**D**) Depletion of NKX3.1 by siRNA in LNCaP cells leads to upregulation of HK2 expression compared with control siLuc (luciferase siRNA) treatment. (**E**) Depletion of NKX3.1 by siRNA in LNCaP-Myc ER cells enhances activation of *HK2* gene expression by tamoxifen (OHT) compared with control siGFP treatment (left panel). In contrast, expression of exogenous Nkx3.1 inhibited OHT induction of Hk2 in DKO cells. Results are representative of at least 2 independent experiments. Error bars represent mean ± SEM. See also Supplemental Figure 4.

Network analysis identifies a gene set coregulated by Nkx3.1 and Myc. To uncover potential relationships between Nkx3.1 target genes, we used the list of direct targets to query the GeneGO MetaCore database (37), which builds gene networks centered on transcription factors. Notably, one of the top ranked networks ($P = 3.94 \times 10^{-169}$) enriched in direct Nkx3.1 target genes was centered on the protooncogene Myc (Figure 4, A and B, and Supplemental Table 5). In addition, 23% of the 282 direct Nkx3.1 targets were also direct Myc targets (Supplemental Table 6). We explored the cellular processes that are regulated by the 65 Nkx3.1/Myc coregulated genes using ClueGO v1.3 (38). ClueGO built a functionally organized network of enriched GO terms using the shared target genes (Supplemental Figure 3). The genes in the established network were enriched in pathways relevant to tumorigenesis, including regulation of telomerase and TNF receptor 2 signaling. These results suggest the intriguing possibility that loss of *Nkx3.1* may promote prostate tumorigenesis by dysregulating a set of cancer-related target genes that are also regulated by Myc.

Identification of Myc targets using GeneGO analysis was based on published binding data (usually ChIP-chip or ChIP-seq) from various cell lines, such as fibroblasts, lymphocytes, and ES cells. To determine whether Myc may regulate shared target genes identified by GeneGO in the prostate, we used ChIP-PCR to validate Myc binding to the shared targets in prostate cancer cells. We used both Myc-CaP, a mouse prostate epithelial cell line derived from Myc transgenic prostate cancer (39), and LNCaP, a human prostate carcinoma cell line derived from a lymph node metastasis (40). Myc-CaP cells expressed Myc but not Nkx3.1, while LNCaP cells expressed both MYC and NKX3.1 (Figure 4, C and D). We confirmed binding of Myc to 7 of 8 sites tested in Myc-CaP cells, including *Hk2*, *Prdx6*, *Txnip*, *Sept9*, *Mt2*, *Mt3*, and *Utrn* (Figure 4C). In LNCaP cells, we observed binding of MYC and NKX3.1 to their respective sites in 7 genes tested by ChIP-qPCR, including *HK2*, *IGF1R*, *PRDX6*, *UTRN*, *ASNS*, *CTSB*, and *HDLP* (Figure 4D).

NKX3.1 opposes MYC's transcriptional activity. NKX3.1 is a tumor suppressor, while MYC is an oncoprotein; therefore, we sought to determine whether NKX3.1 can oppose MYC's transcriptional activity on shared target genes. We first determined whether NKX3.1 could physically interact with MYC. Using coimmunoprecipitation analyses, we showed that MYC and NKX3.1 interacted independently of DNA, as depletion of DNA with ethidium bromide did not abrogate the interaction (Figure 5, A and B). Using deletion mutants of MYC, we found that the interaction between MYC and NKX3.1 was severely reduced when MYC box II was deleted (Figure 5B). To determine whether NKX3.1 and MYC can form a complex at the promoter of shared target genes, we performed sequential ChIP in LNCaP cells. Our analysis at the *HK2* gene E-box (Figure 5C) demonstrated that NKX3.1 and MYC can form a complex at shared target gene promoters. These results suggest

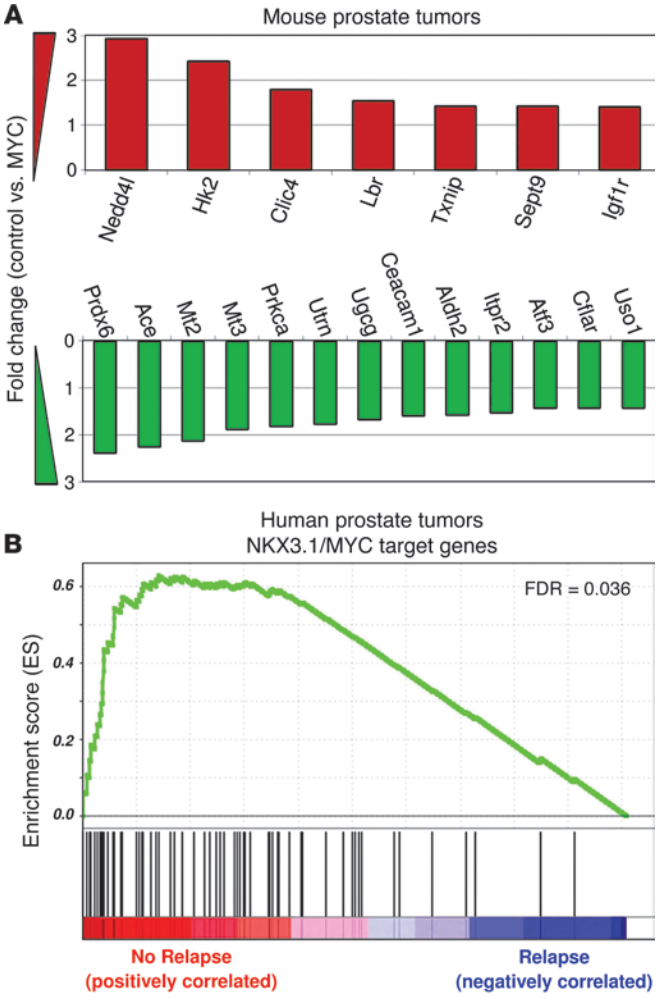

Figure 6
Dysregulation of shared Nkx3.1/MYC target genes in mouse and human prostate cancer tissues. (**A**) Dysregulation of Nkx3.1/MYC targets in a prostate tissue recombination model. Affymetrix arrays were used to compare gene expression between prostate grafts regenerated with mouse prostate epithelial cells transduced with lentivirus overexpressing human MYC or control lentivirus. The MYC grafts contained HGPIN lesions, overexpressed MYC, and downregulated Nkx3.1 (see Supplemental Figure 3). By significance analysis of microarrays (SAM) and employing a 1.4-fold cutoff, 20 of the 65 Nkx3.1/MYC target genes were significantly altered in the grafts containing HGPIN lesions with MYC overexpression and Nkx3.1 downregulation. (**B**) GSEA analysis shows association between expression of NKX3.1/MYC target genes and relapse in human prostate tumors. Gene expression arrays from tumors consisting of 32 tumors with relapse and 34 tumors without relapse were analyzed. See also Supplemental Figures 3 and 5, and Supplemental Tables 5–7.

that NKX3.1 may interact with MYC and modulate MYC's transcriptional activity. Support of this was provided by upregulation of *HK2* gene expression in LNCaP cells when NKX3.1 was depleted by NKX3.1 siRNA (Figure 5D). Furthermore, in LNCaP cells engineered to express the tamoxifen-inducible MycER protein, depletion of NKX3.1 by siRNA enhanced tamoxifen-induced activation of *HK2* gene expression (Figure 5E). Conversely, exogenous Nkx3.1 expression in DKO mouse embryonic fibroblasts (MEFs) expressing MycER impaired the tamoxifen-inducible activation of the *Hk2* gene (Figure 5E and Supplemental Figure 4). Overall, these results indicate that NKX3.1 can antagonize MYC's transcriptional activation of shared target genes.

We next sought to determine whether Nkx3.1 and Myc coregulate target gene expression in prostate tissue in vivo. We examined gene expression microarray data obtained from mouse prostate tissues engineered to overexpress MYC with loss of endogenous Nkx3.1. The MYC-overexpressing prostates were generated using tissue recombination, in which naive adult mouse prostate epithelial cells were transduced with control or MYC-expressing lentivirus, combined with fetal rat urogenital mesenchyme (UGM) and grafted under the renal capsule of intact adult male SCID mice (ref. 41 and Supplemental Figure 5A). We have shown previously that these MYC-expressing grafts at 6 weeks contained multiple foci of high-grade prostatic intraepithelial neoplasia (HGPIN), while control grafts consisted of benign prostate glands (41). In addition, the HGPIN lesions uniformly lost Nkx3.1 protein expression (Supplemental Figure 5B). We performed microarray analysis on MYC grafts (high MYC/low Nkx3.1) and control grafts (i.e., low MYC/high Nkx3.1) to test for dysregulation in shared target genes (42). At the 1.4-fold cutoff, the expression of 20 of 65 MYC/Nkx3.1 shared targets was significantly altered compared with only 2 of 65 randomly selected genes (false discovery rate [FDR] = 0.02; $P = 2.9 \times 10^{-5}$) (Figure 6A). Genes significantly upregulated in MYC grafts (i.e., high MYC/low Nkx3.1) included *Nedd4l*, *Hk2*, *Clic4*, and *Igf1r*, while *Prdx6*, *Ace*, *Mt2*, *Prkca*, *Ugcg*, *Ceacam1*, *Itpr2*, *Cflar*, and *Atf3* were significantly downregulated (Figure 6A). These results indicate that shared Nkx3.1/Myc target genes may be relevant to prostate tumorigenesis in vivo.

We next examined microarray data obtained from LNCaP, PC3, and DU145 cells following MYC knockdown by siRNA (43) for evidence of dysregulation of shared NKX3.1/MYC target genes when Myc is depleted. Using a 1.4-fold cutoff, we found significant dysregulation of shared target genes compared with a randomly generated list of genes in all 3 cell lines (Table 1). We also analyzed the concordance in the direction of target gene expression changes (i.e., up or down) between the human cell line siMYC microarray data and the Myc-overexpressing mouse prostate microarray data (Table 1). The concordance rate was high for the PC3 and DU145 cells (0.67 and 0.75, respectively), but lower (0.4) for LNCaP cells.

Table 1
MYC knockdown dysregulates expression of shared NKX3.1/MYC target genes in human prostate cancer cell lines

	LNCaP	*DU145*	*PC3*
Shared NKX3.1/MYC target genes	11	18	24
Random genes	4	6	9
Concordance with mouse TR	0.4	0.67	0.75
Significance: shared over random	$P = 0.05$	$P = 0.006$	$P = 0.002$

Gene expression microarray data for LNCaP, PC3, and DU145 cells treated with siRNA targeting MYC (43) were examined for alterations in NKX3.1/MYC target genes. There was significant alteration in the expression of the shared NKX3.1/MYC targets compared with a randomly generated list of genes. The concordance in the direction of gene expression changes due to MYC modulation in cell lines was determined, as compared with the MYC-expressing mouse tissue microarray data in Figure 6A. TR, tissue recombinants.

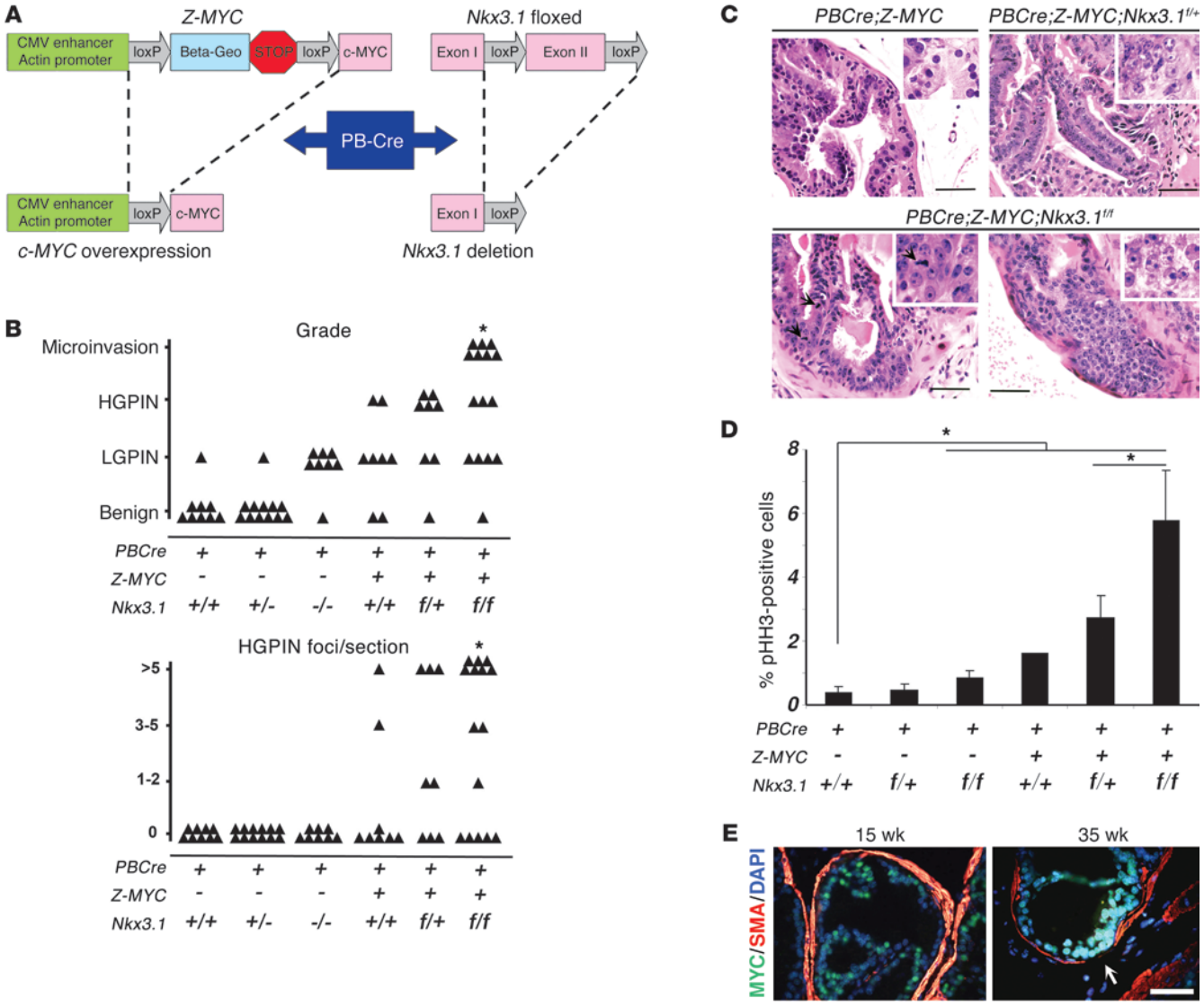

Figure 7

Loss of *Nkx3.1* facilitates MYC-initiated prostate tumorigenesis in transgenic mice. (**A**) Scheme for concurrent overexpression of *MYC* and deletion of *Nkx3.1* in the prostates of transgenic mice. The *Z-MYC* construct contains a latent human *MYC* allele under the control of the CMV enhancer/actin promoter. The floxed allele of *Nkx3.1* has *loxP* sites flanking exon 2, which encodes the *Nkx3.1* homeodomain. Cre recombinase is under the control of the prostate-specific *Probasin* promoter (*PB-Cre*). When Cre is expressed, the *MYC* gene will be overexpressed and the *Nkx3.1* gene will be concurrently deleted. (**B**) Graph summarizing prostate histology of *Nkx3.1/MYC* mutant mice. *$P < 0.01$ for *PBCre;Z-MYC;Nkx3.1$^{f/f}$* relative to *PBCre;Z-MYC*. (**C**) Histological characterization of prostate lesions in *Nkx3.1/MYC* mutant mice. H&E-stained sections of 35-week-old mouse prostates. Note high-grade PIN lesions in *PBCre;Z-MYC;Nkx3.1$^{f/+}$* and *PBCre;Z-MYC;Nkx3.1$^{f/f}$* mice. Insets show higher magnifications (×40). Arrows denote mitotic figures. Scale bars: 50 μm. (**D**) Proliferation in mutant mice prostates assessed by phospho-histone H3 staining. *$P < 0.05$. Error bars represent mean ± SEM. (**E**) Areas of focal loss of SMA (arrows) in 35-week-old *PBCre;Z-MYC;Nkx3.1$^{f/f}$* mice, suggestive of microinvasion. Scale bar: 50 μm. See also Supplemental Figures 6 and 7.

The lower concordance rate in LNCaP cells may be related to the fact that in these cells, MYC knockdown led to a significant alteration in NKX3.1 levels, thereby confounding the analysis.

We extended our analysis to test for dysregulation of NKX3.1/MYC coregulated genes in human prostate cancer. We downloaded raw microarray and clinical data for 66 patients from the NCBI Gene Expression Omnibus (GEO GSE21034) (44). The patients were divided into 2 categories based on presence (32 patients) or absence (34 patients) of biochemical relapse. Using GSEA, we discovered an association between relapse and expression of MYC/NKX3.1 shared target genes (FDR = 0.036). In tumors from patients without relapse, we found significant upregulation of a subset of shared genes (Figure 6B). The specific genes driving this association were found in the leading edge of the gene set and are listed in Supplemental Table 7. Notably, 9 of the 13 genes (70%) downregulated in the Myc-expressing (high Myc/low Nkx3.1) mouse prostate tissues were present in the leading edge of the clinical human array data and upregulated in tumors without

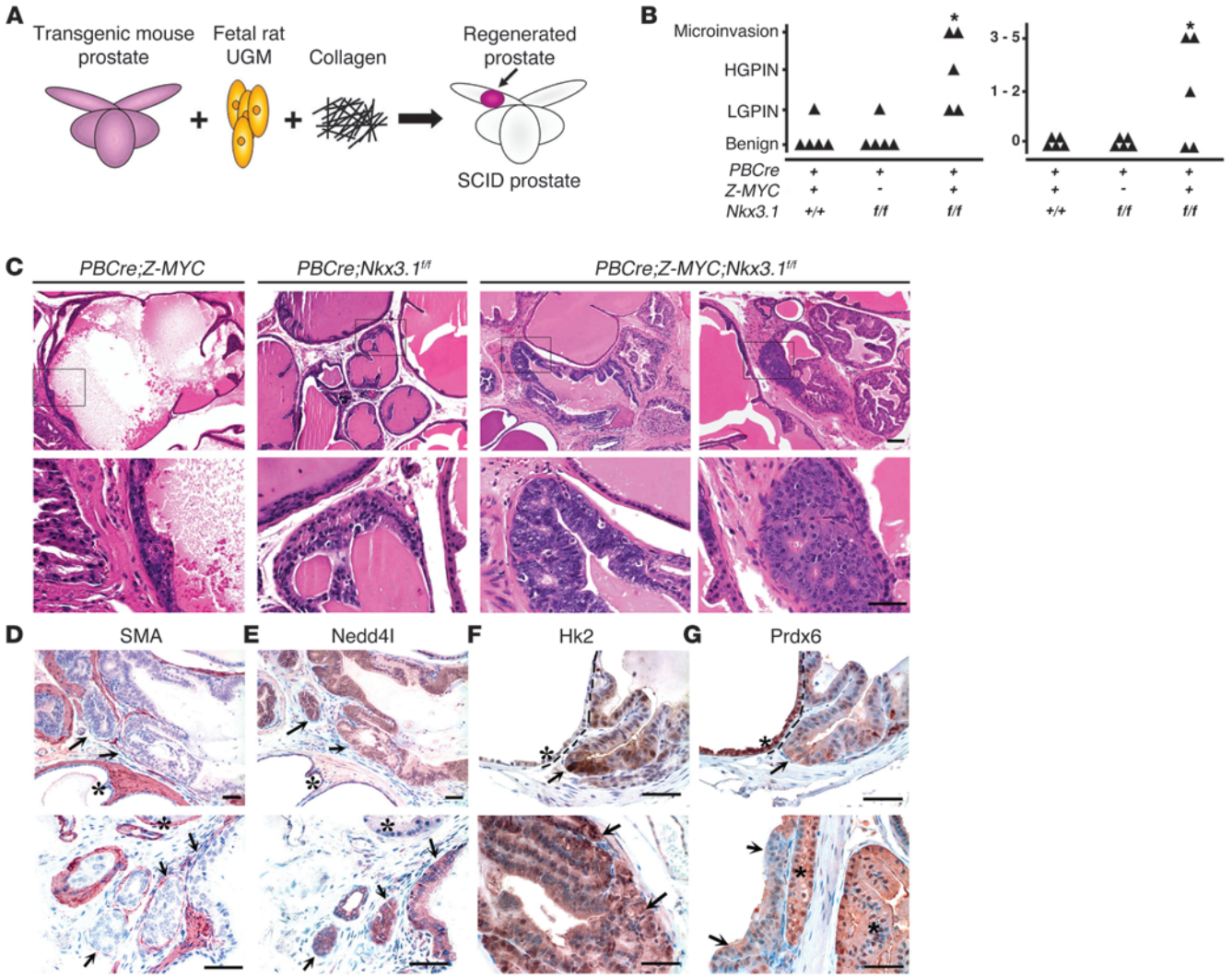

Figure 8

Nkx3.1 and MYC coregulate prostate tumorigenesis and target gene expression. (**A**) Scheme for prostate regeneration by tissue recombination to recapitulate phenotypes of transgenic mice. Pieces of transgenic mouse prostates were combined with rat UGM and collagen and then implanted orthotopically into prostates of SCID mice. Ten weeks later, regenerated prostates were harvested. (**B**) Graph summarizing pathology of regenerated prostates. *$P < 0.05$ for *PBCre;Z-MYC;Nkx3.1*$^{f/f}$ relative to all others. (**C**) Histological characterization of prostate lesions in regenerated prostates. H&E-stained sections of 10-week-old grafts. *PBCre;Z-MYC* and *PBCre;Nkx3.1*$^{f/f}$ grafts show mostly normal glands with areas of hyperplasia and dysplasia consistent with low-grade PIN, while *PBCre;Z-MYC;Nkx3.1*$^{f/f}$ prostates show multiple foci of HGPIN. Scale bars: 50 μm. (**D**) Focal loss of SMA (arrows) consistent with microinvasion in 10-week-old *PBCre;Z-MYC;Nkx3.1*$^{f/f}$ prostate grafts. Asterisks indicate benign glands. Scale bars: 50 μm. (**E**–**G**) Upregulation of Nedd4l and Hk2 and downregulation of Prdx6 expression by immunohistochemistry in HGPIN/cancer lesions from 10-week-old *PBCre;Z-MYC;Nkx3.1*$^{f/f}$ prostate grafts (arrows). Note that the sections in **E** are adjacent to those in **D**. Asterisks indicate benign glands. Scale bars: 50 μm. See also Supplemental Figures 7 and 8.

relapse. These genes included *UGCG*, *MT2A*, *ITPR2*, *CEACAM1*, *ALDH2*, *CFLAR*, *PRKCA*, and *ATF3* (Supplemental Table 7). These results suggest that suppression of these shared target genes due to concerted upregulation of MYC and downregulation of NKX3.1 in tumors may favor relapse.

Nkx3.1 loss cooperates with MYC to promote prostate tumorigenesis. Coregulation of target genes by Nkx3.1 and Myc suggests that Nkx3.1 loss and Myc overexpression may cooperate in prostate tumorigenesis. To test this hypothesis in vivo, we generated transgenic mice with concurrent deletion of mouse *Nkx3.1* and overexpression of human MYC in the mouse prostate. However, prior to undertaking this in vivo study, we addressed 2 possible conceptual concerns that may complicate the interpretation of this experiment. The first concern was that the promoters commonly used to drive prostate-specific transgene expression, such as *Probasin* and *PSA*, are themselves Nkx3.1 target genes. Therefore, *Probasin*-driven *MYC* transgene expression, for example, is likely to be decreased in *Nkx3.1*-deficient prostates. To circumvent this complication, we used Cre/loxP-mediated recombination to concurrently delete endogenous *Nkx3.1* and overexpress MYC in the mouse prostate. Specifically, we crossed *PbCre4;Z-MYC* mice (45, 46) with *Nkx3.1*$^{f/f}$ mice (14). *Z-MYC* is a latent, Cre-activatable *MYC*

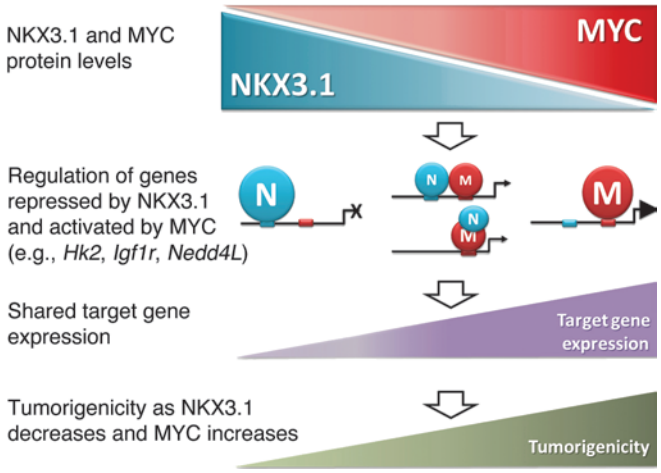

Figure 9

Model for crossregulation of prostate tumorigenesis by convergence of NKX3.1 and MYC on shared target genes. NKX3.1 and MYC protein levels vary during tumorigenesis, ranging from low MYC/high NKX3.1 in benign tissue to high MYC/low NKX3.1 in more advanced tumors. In benign tissue, where NKX3.1 protein levels are high and MYC levels are very low, shared target genes such as *HK2* are bound and repressed by NKX3.1. In samples in which both NKX3.1 and MYC are expressed, NKX3.1 can bind to its consensus DNA site as well as form a complex with MYC to dampen MYC's transcriptional activity and target gene expression. In advanced tumors, where MYC is highly expressed and NKX3.1 expression lost, MYC binds and activates its target genes unopposed. Thus, as tumorigenesis progresses, the MYC:NKX3.1 ratio increases and the expression of protumorigenic shared target genes (activated by MYC and repressed by NKX3.1) increases. In the model depicted here, we show NKX3.1 as a transcriptional repressor and MYC as an activator of protumorigenic target genes. However, the converse, where NKX3.1 activates and MYC represses antitumorigenic target genes, also fits the general model. See also Supplemental Figure 9.

allele. Thus, prostate-specific Cre expression resulted in concurrent deletion of *Nkx3.1* and activation of *MYC* expression (Figure 7A). Because the activated *MYC* transgene is under the control of the CMV enhancer/actin promoter, loss of *Nkx3.1* should not affect transgene expression.

The second concern is that MYC may directly repress *Nkx3.1* expression (47), in which case deleting *Nkx3.1* would have no added advantage to MYC overexpression in prostate cells. We examined this possibility by double staining *PBCre;Z-MYC* transgenic mouse prostates for MYC and Nkx3.1. While some MYC-overexpressing cells showed evidence of reduced Nkx3.1 expression, we observed a number of cells coexpressing MYC and Nkx3.1 (Supplemental Figure 6A). Staining of adjacent serial sections for MYC and Nkx3.1 also showed similar results (Supplemental Figure 6B). Therefore, in this model, MYC overexpression does not immediately lead to downregulation of Nkx3.1 protein expression. These results are consistent with our previous observations showing that MYC overexpression in *PBCre;Z-MYC* mice sensitizes cells to transformation, but does not by itself lead to significant pathology, contrary to the case in *Probasin-MYC* mice (46–48). This may be related to differences in background strains or MYC expression levels (47). In sum, our results indicate that the *PBCre;Z-MYC* model is well suited for determining whether *Nkx3.1* deletion will modify MYC-induced prostate tumorigenesis in vivo.

We characterized prostate tumorigenesis in cohorts of conditional *MYC/Nkx3.1* mutant mice. Prostate-specific deletion of *Nkx3.1* using the *PBCre4* line resulted in epithelial hyperplasia and dysplasia (Supplemental Figure 7A), similar to what has been observed using a *PSA-Cre* line (14). Focal prostate expression of MYC in *PbCre4;Z-MYC* mice resulted in mild pathology (Figure 7, B and C) as reported earlier (46). Notably, cooperativity between Nkx3.1 loss and MYC overexpression was evident as early as 15 weeks of age in *PbCre4;Z-MYC;Nkx3.1*$^{f/+}$ and *PbCre4;Z-MYC;Nkx3.1*$^{f/f}$ mice, with 62% and 67% developing focal HGPIN lesions, respectively (Figure 7, B and C). Strikingly, 70% of the *PbCre4;Z-MYC;Nkx3.1*$^{f/f}$ HGPIN lesions developed microinvasive cancer (Figure 7, B and E). Over time, the density of multifocal HGPIN lesions increased to more than 5 foci per section in *PbCre4;Z-MYC;Nkx3.1*$^{f/f}$ mice (Figure 7B). As shown in Figure 7D, proliferation was significantly increased in *PbCre4;Z-MYC;Nkx3.1*$^{f/+}$ and *PbCre4;Z-MYC;Nkx3.1*$^{f/f}$ prostates, while apoptosis showed a modest increase (S.A. McKissic and S.A. Abdulkadir, unpublished observations).

We extended these results by prostate regeneration using tissue recombination. Prostates regenerated by tissue recombination recapitulate the prostate phenotypes of transgenic mice (49), with the added benefits of savings in time and cost. In this assay (Figure 8A), we combined pieces of adult transgenic mouse prostate tissue with fetal UGM. Tissue recombinants were then grafted orthotopically into the anterior prostates of SCID mice. Then, 6 or 10 weeks later, grafts containing regenerated prostates were harvested. Regenerated glands can be distinguished from host SCID mouse prostate glands by MYC expression and/or loss of Nkx3.1 expression (Supplemental Figure 7C). Histological examination of grafts showed that while *PbCre4;Z-MYC* and *PbCre4;Nkx3.1*$^{f/f}$ grafts were either histologically normal or developed epithelial hyperplasia and LGPIN, grafts from *PbCre4;Z-MYC;Nkx3.1*$^{f/f}$ mice contained HGPIN lesions with microinvasive cancer (Figure 8, B–D, and Supplemental Figure 7D). We next sought to determine whether the expression of Nkx3.1/MYC coregulated genes was altered in *Nkx3.1/MYC* mutant mice. Using immunohistochemistry, we examined the expression of Hexokinase 2 (Hk2), a key glycolic isoenzyme, Nedd4l, an E3 ubiquitin ligase, and Prdx6, an antioxidant enzyme, in prostate tissue sections from *PbCre4;Z-MYC;Nkx3.1*$^{f/f}$ mouse grafts. We observed significant upregulation of Hk2 and Nedd4l and downregulation of Prdx6 proteins in the HGPIN/microinvasive carcinoma lesions (Figure 8, E–G, and Supplemental Figure 8). These results support a role for these coregulated target genes in prostate tumorigenesis.

Discussion

In this work, we found significant overlap between targets of the prostate tumor suppressor Nkx3.1 and Myc using integrated genomic analysis. Prior to this study, few direct targets of the Nkx3.1 tumor suppressor were known. By integrating ChIP-seq and gene expression data, we defined a set of 282 direct target genes both bound and regulated by Nkx3.1. This number probably represents an underestimate, given the use of older platforms in the 2 microarray studies that catalogued genes with dysregulated expressions in the prostates of *Nkx3.1* mice (31, 32).

It is notable that Nkx3.1 binding is enriched near genes, particularly around 150 nt upstream of the TSS. Nkx3.1 has been implicated in regulating the production of secretions in the differentiated prostate, and we found that Nkx3.1-bound genes were enriched in processes relevant to this function, including amino

acyl-tRNA synthesis, amino acid metabolism, and regulation of oxidative stress. The availability of the Nkx3.1 cistrome enabled us to refine the in vivo consensus Nkx3.1-binding motif from TAAGTA to AAGTW and provides the scientific community with a comprehensive resource for further investigation of Nkx3.1 function in specific cell types. For example, Nkx3.1 has been implicated in regulating self renewal of specific types of prostate stem cells called castration-resistant Nkx3.1-expressing cells (CARNs) and in regulating T cell lymphomagenesis (6, 50). In these settings, Nkx3.1 may regulate a distinct set of genes compared with those it regulates in differentiated prostate epithelium.

It is striking that many of the direct Nkx3.1 targets are also targets of the Myc oncoprotein. Several of these "shared" Nkx3.1/Myc targets have been implicated in various aspects of tumorigenesis. For example, Hk2, a key glycolytic enzyme, is involved in promoting the Warburg effect and tumorigenesis in cancer cells (51). The E3 ubiquitin ligase Nedd4l, which is involved in targeting components of the TGF-β pathway for degradation, was found in some studies to be upregulated in prostate cancer (52). It is likely that dysregulation of multiple Nkx3.1/Myc target genes contributes to malignant transformation. Myc is a well-known regulator of proliferation, differentiation, and tumorigenesis (53). Thus, some of the consequences of Nkx3.1 loss in the prostate, including hyperproliferation and dedifferentiation (5, 14), may be achieved via direct dysregulation of the shared targets. In human prostate cancer, overexpression of MYC is an early and frequent event (41, 54). The expression of NKX3.1 is also often reduced in human prostate tumors (22, 55), and an inherited variant of the *NKX3.1* gene with reduced expression is associated with increased risk of prostate cancer (12).

Based on our studies, we propose the following model to explain the relationship between NKX3.1 and MYC in prostate tumorigenesis (Figure 9). The levels of NKX3.1 and MYC vary in tumorigenesis, with the MYC:NKX3.1 ratio increasing with progression. Our data suggest that NKX3.1 and MYC directly bind and coregulate a common subset of target genes relevant to prostate tumorigenesis (Supplemental Figure 9). We propose that NKX3.1 opposes MYC's transcriptional activity. Thus, as the MYC:NKX3.1 ratio increases, MYC's transactivation of protumorigenic target genes (such as HK2, IGF1R, NEDD4L) increases, thereby promoting tumorigenesis. In the case of antitumorigenic target genes (e.g., *ACE*, *MT2*) that are repressed by MYC and activated by NKX3.1, the converse is true. As the MYC:NKX3.1 ratio increases, the expression of these target genes will decrease, enhancing tumorigenesis.

Although our study focused on how Nkx3.1 modulates Myc function, Myc may also modulate Nkx3.1 function. Nkx3.1 and Myc may modulate each other's transcriptional activity in several ways. For example, Nkx3.1 and Myc may affect each other's recruitment to chromatin. Alternatively, binding of Nkx3.1 to promoters/enhancers may affect Myc's transactivation function by interfering with Myc's ability to assemble an active transcription initiation complex. The converse may also be true for target genes that are repressed by Myc. Additional studies are needed to examine these possibilities. Myc's transactivation function may be modulated by complex formation with other factors on chromatin. For example, p19ARF could associate with Myc on chromatin, opposing the transactivation of selected Myc target genes (56, 57). Myc can also be recruited to promoter regions via binding to the transcription factor MIZ-1 to repress expression of some target genes (58, 59). Finally, although not all shared target genes are coordinately regulated by Myc and Nkx3.1, our analysis provides evidence for cooperation between Myc overexpression and Nkx3.1 loss in promoting cancer and dysregulating multiple shared target genes known to be involved in tumorigenesis. The type of interaction we identified between MYC and Nkx3.1, whereby 2 transcription factors converge to crossregulate common target genes, may provide a mechanistic basis for some oncogene/TSG cooperativity.

Methods

Mice. *Nkx3.1*$^{-/-}$, *Nkx3.1*$^{f/f}$, and *PBcre4;Z-MYC* mice have been described (14, 45, 46). Alleles were maintained on a recombinant inbred BL6/129 background. *Nkx3.1*$^{+/-}$ mice were brother-sister–mated to produce the males used in this study.

ChIP-seq assays. Whole prostates from *Nkx3.1*$^{+/+}$, *Nkx3.1*$^{+/-}$, and *Nkx3.1*$^{-/-}$ mice at 12 to 16 weeks of age were used. Initial ChIP using anti-Nkx3.1 antibody (sc-15022; Santa Cruz Biotechnology Inc.) was performed by Genpathway. HudsonAlpha performed deep sequencing. The genome coordinates of each read were inferred based on sequence homology to mouse genome build 37. Peaks were called using the model-based analysis of ChIP-seq (MACS) algorithm (19) using the KO sample as a control for nonspecific *Nkx3.1* antibody binding. Further details on ChIP assay can be found in the Supplemental Methods.

Binding site motif analysis. We used Genomatix MatInspector (24) to search 1,000 randomly selected Nkx3.1 intervals for known transcription factor–binding sites. In addition, we performed de novo motif discovery using MEME 4.6.0 (30). The MEME settings were as follows: 1 motif per sequence (OOPS model), minimum motif width = 6, maximum motif width = 20. To search for the AAGTW Nkx3.1 motif in Nkx3.1-bound intervals, peaks were divided into 10 quantiles based on their amplitude. Q1 had the tallest peaks and Q10 the shortest. FIMO (part of MEME suite 4.6.0) was used to search significant ChIP-seq intervals for the consensus Nkx3.1 motif that was discovered using MEME. All sequences were screened using RepeatMasker (version 3.2.9) before analysis using the mouse repeat libraries (RepBase 2009-06-04; Genetic Information Research Institute).

Network analysis. The 282 direct Nkx3.1 target genes were uploaded into the MetaCore analytical suite (GeneGO) and analyzed as described previously (37). We built networks centered on transcription factors such that subnetworks centered on transcription factors were generated, with subnetworks ranked by a *P* value and a G score. Subnetworks were also interpreted in terms of GO.

GSEA. For *Nkx3.1* mutant mice, the curated gene sets of the Molecular Signatures Database (MSigDB version 2.5) were tested for enrichment in robust multichip averaging–normalized (RMA-normalized) microarray expression data from a previously published microarray study (31). For human tumors, we obtained raw gene expression microarray data with matching clinical data for 66 human prostate adenocarcinoma patients from Gene Expression Omnibus (GEO GSE21034) (44). The microarray data were processed and converted to RMA-normalized expression values in Bioconductor using XPS. The patients were divided into 2 populations based on presence (32 patients) or absence (34 patients) of biochemical relapse within 5 years. GSEA v2.07 (33) was used to test for expression changes in a gene set consisting of 65 NKX3.1/MYC coregulated genes.

Prostate regeneration by tissue recombination. This was performed generally as described before (41). Briefly, 8- to 10-week-old *PBCre;Z-MYC*, *PBCre;Nkx3.1*$^{f/f}$, or *PBCre;Z-MYC;Nkx3.1*$^{f/f}$ mouse prostate tissues were minced, combined with freshly isolated fetal rat UGM cells, and incubated in collagen overnight. The next day, tissue recombinants were grafted under the capsule of 1 anterior prostate lobe of 7- to 8-week-old SCID mice and, 6 or 10 weeks later, grafts were harvested.

Statistics. We employed the hypergeometric test, Fisher's exact test, and the 2-tailed Student's *t* test for statistical analysis. $P \leq 0.05$ was considered significant. Unless indicated otherwise, error bars represent mean ± SEM.

Study approval. All procedures were approved by the Vanderbilt University Institutional Animal Care and Use Committee (IACUC).

Accession numbers. The short-read sequencing data have been deposited in the National Center for Biotechnology Short Read Archive (GEO GSE35971).

Acknowledgments

We thank Pia Arrate and Erin Martinez for technical assistance. This work was supported by grants CA094858 and CA123484 from the National Cancer Institute (NCI) and W81XWH-09-1-0439 from the Department of Defense (DoD) (to S.A. Abdulkadir). C.M. Eischen was supported by CA148950, and S.W. Hayward was supported by U54 CA126505 from the NCI. P.D. Anderson was supported by a DoD postdoctoral fellowship award (W81XWH-11-1-0230). S.A. McKissic was supported by award 3R01CA094858-07S1 from the National Cancer Institute. The content is solely the responsibility of the authors and does not necessarily represent the official views of the National Cancer Institute or the NIH.

Received for publication April 15, 2011, and accepted in revised form February 22, 2012.

Address correspondence to: Sarki Abdulkadir, Department of Pathology, Microbiology and Immunology, 1161 21st Ave. South, B-MCN-3321A, Nashville, Tennessee 37232, USA. Phone: 615.322.9668; Fax: 615.322.7023; E-mail: sarki.abdulkadir@vanderbilt.edu.

1. Land H, Parada LF, Weinberg RA. Tumorigenic conversion of primary embryo fibroblasts requires at least two cooperating oncogenes. *Nature*. 1983;304(5927):596–602.
2. Ruley HE. Adenovirus early region 1A enables viral and cellular transforming genes to transform primary cells in culture. *Nature*. 1983;304(5927):602–606.
3. McMurray HR, et al. Synergistic response to oncogenic mutations defines gene class critical to cancer phenotype. *Nature*. 2008;453(7198):1112–1116.
4. Luo J, Elledge SJ. Cancer: Deconstructing oncogenesis. *Nature*. 2008;453(7198):995–996.
5. Bhatia-Gaur R, et al. Roles for Nkx3.1 in prostate development and cancer. *Genes Dev*. 1999; 13(8):966–977.
6. Wang X, et al. A luminal epithelial stem cell that is a cell of origin for prostate cancer. *Nature*. 2009;461(7263):495–500.
7. Abdulkadir SA. Mechanisms of prostate tumorigenesis: roles for transcription factors Nkx3.1 and Egr1. *Ann N Y Acad Sci*. 2005;1059:33–40.
8. Abate-Shen C, Shen MM, Gelmann E. Integrating differentiation and cancer: the Nkx3.1 homeobox gene in prostate organogenesis and carcinogenesis. *Differentiation*. 2008;76(6):717–727.
9. Zheng SL, et al. Germ-line mutation of NKX3.1 cosegregates with hereditary prostate cancer and alters the homeodomain structure and function. *Cancer Res*. 2006;66(1):69–77.
10. Eeles RA, et al. Identification of seven new prostate cancer susceptibility loci through a genome-wide association study. *Nat Genet*. 2009;41(10):1116–1121.
11. Takata R, et al. Genome-wide association study identifies five new susceptibility loci for prostate cancer in the Japanese population. *Nat Genet*. 2010;42(9):751–754.
12. Akamatsu S, et al. A functional variant in NKX3.1 associated with prostate cancer susceptibility down-regulates NKX3.1 expression. *Hum Mol Genet*. 2010;19(21):4265–4272.
13. Kim MJ, et al. Nkx3.1 mutant mice recapitulate early stages of prostate carcinogenesis. *Cancer Res*. 2002;62(11):2999–3004.
14. Abdulkadir SA, et al. Conditional loss of nkx3.1 in adult mice induces prostatic intraepithelial neoplasia. *Mol Cell Biol*. 2002;22(5):1495–1503.
15. Kim MJ, et al. Cooperativity of Nkx3.1 and Pten loss of function in a mouse model of prostate carcinogenesis. *Proc Natl Acad Sci U S A*. 2002;99(5):2884–2889.
16. Abate-Shen C, et al. Nkx3.1; Pten mutant mice develop invasive prostate adenocarcinoma and lymph node metastases. *Cancer Res*. 2003; 63(14):3886–3890.
17. Wang S, et al. Prostate-specific deletion of the murine Pten tumor suppressor gene leads to metastatic prostate cancer. *Cancer Cell*. 2003;4(3):209–221.
18. Lei Q, et al. NKX3.1 stabilizes p53, inhibits AKT activation, and blocks prostate cancer initiation caused by PTEN loss. *Cancer Cell*. 2006;9(5):367–378.
19. Zhang Y, et al. Model-based analysis of ChIP-Seq (MACS). *Genome Biol*. 2008;9(9):R137.
20. Mogal AP, van der Meer R, Crooke PS, Abdulkadir SA. Haploinsufficient prostate tumor suppression by Nkx3.1: a role for chromatin accessibility in dosage-sensitive gene regulation. *J Biol Chem*. 2007;282(35):25790–25800.
21. He WW, et al. A novel human prostate-specific, androgen-regulated homeobox gene (NKX3.1) that maps to 8p21, a region frequently deleted in prostate cancer. *Genomics*. 1997;43(1):69–77.
22. Bowen C, et al. Loss of NKX3.1 expression in human prostate cancers correlates with tumor progression. *Cancer Res*. 2000;60(21):6111–6115.
23. O'Geen H, et al. Genome-wide binding of the orphan nuclear receptor TR4 suggests its general role in fundamental biological processes. *BMC Genomics*. 2010;11:689.
24. Cartharius K, et al. MatInspector and beyond: promoter analysis based on transcription factor binding sites. *Bioinformatics*. 2005;21(13):2933–2942.
25. Wang Q, et al. A hierarchical network of transcription factors governs androgen receptor-dependent prostate cancer growth. *Mol Cell*. 2007;27(3):380–392.
26. Lupien M, et al. FoxA1 translates epigenetic signatures into enhancer-driven lineage-specific transcription. *Cell*. 2008;132(6):958–970.
27. He HH, et al. Nucleosome dynamics define transcriptional enhancers. *Nat Genet*. 2010;42(4):343–347.
28. Yu J, et al. An integrated network of androgen receptor, polycomb, and TMPRSS2-ERG gene fusions in prostate cancer progression. *Cancer Cell*. 2010;17(5):443–454.
29. Steadman DJ, Giuffrida D, Gelmann EP. DNA-binding sequence of the human prostate-specific homeodomain protein NKX3.1. *Nucleic Acids Res*. 2000;28(12):2389–2395.
30. Bailey TL, Elkan C. Fitting a mixture model by expectation maximization to discover motifs in biopolymers. *Proc Int Conf Intell Syst Mol Biol*. 1994;2:28–36.
31. Magee JA, Abdulkadir SA, Milbrandt J. Haploinsufficiency at the Nkx3.1 locus. A paradigm for stochastic, dosage-sensitive gene regulation during tumor initiation. *Cancer Cell*. 2003;3(3):273–283.
32. Ouyang X, DeWeese TL, Nelson WG, Abate-Shen C. Loss-of-function of Nkx3.1 promotes increased oxidative damage in prostate carcinogenesis. *Cancer Res*. 2005;65(15):6773–6779.
33. Subramanian A, et al. Gene set enrichment analysis: a knowledge-based approach for interpreting genome-wide expression profiles. *Proc Natl Acad Sci U S A*. 2005;102(43):15545–15550.
34. Kanehisa M, Goto S. KEGG: kyoto encyclopedia of genes and genomes. *Nucleic Acids Res*. 2000; 28(1):27–30.
35. Weigel AL, Handa JT, Hjelmeland LM. Microarray analysis of H2O2-, HNE-, or tBH-treated ARPE-19 cells. *Free Radic Biol Med*. 2002;33(10):1419–1432.
36. Zhang B, Kirov S, Snoddy J. WebGestalt: an integrated system for exploring gene sets in various biological contexts. *Nucleic Acids Res*. 2005;33(web server issue):W741–W748.
37. Nikolsky Y, Nikolskaya T, Bugrim A. Biological networks and analysis of experimental data in drug discovery. *Drug Discov Today*. 2005;10(9):653–662.
38. Bindea G, et al. ClueGO: a Cytoscape plug-in to decipher functionally grouped gene ontology and pathway annotation networks. *Bioinformatics*. 2009;25(8):1091–1093.
39. Watson PA, Ellwood-Yen K, King JC, Wongvipat J, Lebeau MM, Sawyers CL. Context-dependent hormone-refractory progression revealed through characterization of a novel murine prostate cancer cell line. *Cancer Res*. 2005; 65(24):11565–11571.
40. Horoszewicz JS, et al. LNCaP model of human prostatic carcinoma. *Cancer Res*. 1983;43(4):1809–1818.
41. Wang J, et al. Pim1 kinase synergizes with c-MYC to induce advanced prostate carcinoma. *Oncogene*. 2010;29(17):2477–2487.
42. Wang J, Anderson PD, Luo W, Gius D, Roh M, Abdulkadir SA. Pim1 kinase is required to maintain tumorigenicity in MYC-expressing prostate cancer cells [published online ahead of print August 22, 2011]. *Oncogene*. doi:10.1038/onc.2011.371.
43. Koh CM, et al. Alterations in nucleolar structure and gene expression programs in prostatic neoplasia are driven by the MYC oncogene. *Am J Pathol*. 2011;178(4):1824–1834.
44. Taylor BS, et al. Integrative genomic profiling of human prostate cancer. *Cancer Cell*. 2010; 18(1):11–22.
45. Roh M, Kim J, Song C, Wills M, Abdulkadir SA. Transgenic mice for Cre-inducible overexpression of the oncogenes c-MYC and Pim-1 in multiple tissues. *Genesis*. 2006;44(10):447–453.
46. Kim J, Eltoum IE, Roh M, Wang J, Abdulkadir SA. Interactions between cells with distinct mutations in c-MYC and Pten in prostate cancer. *PLoS Genet*. 2009;5(7):e1000542.
47. Iwata T, et al. MYC overexpression induces prostatic intraepithelial neoplasia and loss of Nkx3.1 in mouse luminal epithelial cells. *PLoS One*. 2010;5(2):e9427.
48. Ellwood-Yen K, et al. Myc-driven murine prostate cancer shares molecular features with human prostate tumors. *Cancer Cell*. 2003;4(3):223–238.
49. Ishii K, Shappell SB, Matusik RJ, Hayward SW. Use of tissue recombination to predict phenotypes of transgenic mouse models of prostate carcinoma. *Lab Invest*. 2005;85(9):1086–1103.
50. Kusy S, et al. NKX3.1 is a direct TAL1 target gene that mediates proliferation of TAL1-expressing human T cell acute lymphoblastic leukemia. *J Exp Med*. 2010;207(10):2141–2156.

51. Mathupala SP, Ko YH, Pedersen PL. Hexokinase-2 bound to mitochondria: cancer's stygian link to the "Warburg Effect" and a pivotal target for effective therapy. *Semin Cancer Biol*. 2009;19(1):17–24.
52. Hellwinkel OJ, et al. Transcription alterations of members of the ubiquitin-proteasome network in prostate carcinoma. *Prostate Cancer Prostatic Dis*. 2011;14(1):38–45.
53. Dang CV, O'Donnell KA, Zeller KI, Nguyen T, Osthus RC, Li F. The c-Myc target gene network. *Semin Cancer Biol*. 2006;16(4):253–264.
54. Gurel B, et al. Nuclear MYC protein overexpression is an early alteration in human prostate carcinogenesis. *Mod Pathol*. 2008;21(9):1156–1167.
55. Bethel CR, et al. Decreased NKX3.1 protein expression in focal prostatic atrophy, prostatic intraepithelial neoplasia, and adenocarcinoma: association with gleason score and chromosome 8p deletion. *Cancer Res*. 2006;66(22):10683–10690.
56. Qi Y, Gregory MA, Li Z, Brousal JP, West K, Hann SR. p19ARF directly and differentially controls the functions of c-Myc independently of p53. *Nature*. 2004;431(7009):712–717.
57. Datta A, et al. Myc-ARF (alternate reading frame) interaction inhibits the functions of Myc. *J Biol Chem*. 2004;279(35):36698–36707.
58. Seoane J, Pouponnot C, Staller P, Schader M, Eilers M, Massague J. TGFbeta influences Myc, Miz-1 and Smad to control the CDK inhibitor p15INK4b. *Nat Cell Biol*. 2001;3(4):400–408.
59. Staller P, et al. Repression of p15INK4b expression by Myc through association with Miz-1. *Nat Cell Biol*. 2001;3(4):392–399.